2 Theories, Models and Methods

Parts of this chapter previously appeared as

Activation Strain Model & Molecular Orbital Theory
L. P. Wolters, F. M. Bickelhaupt
WIREs Comput. Mol. Sci. **2015**, *5*, 324–343

2.1 Semantics

The terms 'theory' and 'model' are regularly used throughout this thesis. Before proceeding with a more detailed discussion of the specific theories and models applied in this work, it is therefore appropriate to give some attention to the meaning of these terms, as this is often a source of confusion. The purpose of this brief section is not to provide a thorough and definitive view on theories and models and their application within the scientific method. Instead, it is meant as a word of caution, that should be in the back of one's mind when reading the brief explanation of the theories and models as applied within this thesis, and especially when discussing the interpretation of data in the following chapters.

Probably the most common example of misunderstanding the scientific term 'theory' is a creationist pointing out that "*the biological theory of evolution is just a theory*". This is a non-sensical statement, because it fallaciously equivocates on two different (in fact, almost opposite) meanings of the term 'theory'. In this argument the term is used in its colloquial sense, which in the Oxford English Dictionary is described as "*a hypothesis proposed as an explanation; hence, a mere hypothesis, speculation, conjecture; an idea or set of ideas about something; an individual view or notion*".[134] But in the case of the 'theory of evolution', the term refers to a scientific theory, which is aptly described by the American Association for the Advancement of Science as "*a well-substantiated explanation of some aspect of the natural world, based on a body of facts that have been repeatedly confirmed through observation and ex-*

periment".[135] A creationist might argue that this latter definition does not apply to evolution, but, apart from being factually wrong, that is not the point the initial statement was intended to make.

The results within this thesis are largely obtained using density functional theory. Density functional theory itself does not directly explain anything, and therefore does not fit any of the definitions given above. Instead, 'theory' here refers to a mathematical framework, derived from a set of postulates, which is intended to make predictions of physical results. In the case of density functional theory, it aims at reproducing the exact electronic density of a molecular fragment, from which physical properties of the fragment can be derived.

Within the scientific community, most of the discussions result not from this ambiguity of the word 'theory', but because of different views on the applied models. Models are used to interpret the data obtained from, for example, density functional theory. A model, within scientific context, is "*a simplified or idealized description of a particular system, situation, or process, often in mathematical terms, that is put forward as a basis for theoretical or empirical understanding*".[136] Within the field of theoretical chemistry, there are many discussions centered around the use of models. Given that a model is an idealized, often simplified description, and therefore inherently false, it should be judged on the basis of its usefulness: the quality of its predictions, general applicability, ease of understanding, etc. Interestingly, however, many of these discussions focus on the truth of particular individual components of a model, such as the different energy components in the interaction energy decomposition scheme discussed in section 2.6. It is therefore often not the model itself that is causing the debate, but rather the overinterpretation of its results.

2.2 Quantum Chemistry

The goal of quantum chemistry is to obtain insight into a molecular system by solving the Schrödinger equation,[137] which in the non-relativistic, time-independent form is[138-140]

$$H\Psi = E\Psi \,. \tag{2.1}$$

In this equation, the Hamiltonian operator H represents the total energy of a system of atomic nuclei and electrons, of which the quantum mechanical motions are described by the wavefunction Ψ. The Hamiltonian includes terms for the kinetic energy of all nuclei N (T_N) and electrons e (T_e), as well as potential energy terms to describe the electrostatic at-

traction between nuclei and electrons (V_{Ne}), and the repulsive nucleus-nucleus (V_{NN}) and electron-electron interactions (V_{ee}):

$$H = T_N + T_e + V_{NN} + V_{Ne} + V_{ee} \,. \tag{2.2}$$

According to the postulates of quantum mechanics, the wavefunction Ψ contains all information about the state of the system it describes. Unfortunately, this equation can only be solved exactly for one-electron atoms. Most chemical problems, of course, involve many more atoms and electrons, and require approximations to obtain solutions. The most regularly applied approximation is the Born-Oppenheimer approximation, which is based on the significant mass difference between the nuclei and electrons (the mass of a proton is roughly 1800 times that of an electron). Thus, the nuclei move much slower than electrons, and the electrons are therefore assumed to move around fixed nuclei. Effectively, the kinetic energy of the nuclei is then zero, the nucleus-nucleus repulsion is reduced to a constant, and the electrons experience a fixed potential from the positively charged nuclei. The Hamiltonian in Equation 2.2 then reduces to the electronic Hamiltonian H_{elec}, working on the electronic wavefunction Ψ_{elec}:

$$H_{elec}\Psi_{elec} = (T_e + V_{Ne} + V_{ee})\Psi_{elec} \,. \tag{2.3}$$

The electronic wavefunction Ψ_{elec} is usually approximated as an antisymmetric product of one-electron wavefunctions, such as in the Hartree-Fock scheme. Using this scheme, it is possible to recover roughly 99% of the total energy of the molecular system. Most importantly, it is missing a large part of V_{ee} because the correlation of the movements of electrons is not completely accounted for. Unfortunately, total energies are large quantities and chemists are generally interested in energy changes that are of the order of magnitude of the remaining 1%, or even smaller. More elaborate schemes, such as the configuration interaction (CI) method, or the coupled cluster (CC) method, are based on similar principles as Hartree-Fock, but have superior accuracy due to an improved approximation of the wavefunction.

2.3 Density Functional Theory

Instead of attempting to improve the wavefunction, as is done in wavefunction theory, a different approach has led to the development of density functional theory (DFT).[141,142] Its essential basis is a theorem proven by Hohenberg and Kohn,[143] which states that the

electron density ρ uniquely determines all properties of the molecular system, including the electronic energy:

$$E = E[\rho] \,. \tag{2.4}$$

Thus, the electronic energy has a functional dependence on the electron density, which is a function of only 3 spatial variables. This translates into a considerable reduction in computational cost compared to wavefunction methods, where the electronic energy has a functional dependence on the electronic wavefunction, which contains three spatial variables for each electron (and a fourth variable if spin is taken into account).

A practical approach to put this idea to work has been provided by Kohn and Sham.[144] They introduced the concept of a reference system of non-interacting electrons, moving in an effective potential V_S. This Kohn-Sham potential is constructed such that the density of the reference system equals the density of the real, interacting system. Thus, in Kohn-Sham DFT, the electronic wavefunction of the reference system is expressed by a single Slater determinant, consisting of one-electron wavefunctions. These wavefunctions are the Kohn-Sham orbitals φ, from which the electron density can be constructed by taking a linear combination of their densities:

$$\rho(r) = \sum_i |\varphi_i|^2 \,. \tag{2.5}$$

The electronic energy is obtained from the density by the energy functional

$$E[\rho(r)] = T_S[\rho(r)] + E_{Ne}[\rho(r)] + E_C[\rho(r)] + E_{XC}[\rho(r)] \,. \tag{2.6}$$

The first term in this expression, $T_S[\rho(r)]$, describes the kinetic energy of the electrons in the non-interacting reference system. $E_{Ne}[\rho(r)]$ represents the electrostatic attraction between the electron density and the nuclei. The third term, $E_C[\rho(r)]$, is the classical Coulomb repulsion between the electrons, that is, the repulsion each electron experiences from the average field due to all electrons, including itself. The final term, $E_{XC}[\rho(r)]$ is the exchange-correlation energy, which corrects for the deficiencies of $T_S[\rho(r)]$ and $E_C[\rho(r)]$. The kinetic energy of the electrons in the Kohn-Sham reference system, $T_S[\rho(r)]$, is different from the kinetic energy of the real system, $T[\rho(r)]$. For the third term, $E_C[\rho(r)]$, there are a number of deficiencies that have to be corrected. Firstly, electrons do not repel themselves, thus, the Coulomb repulsion computed from the average field of all electrons, contains a self-interaction error. Secondly, following from the Pauli exclusion principle, the probability of finding two same-spin electrons at the same point in space should be zero. Thirdly,

the motions of electrons are correlated: they avoid each other due to mutual Coulomb repulsion. Unfortunately, the form of the exchange-correlation functional is not known exactly, and has to be approximated. Nowadays, there is an incredible amount of functionals to choose from, and a large number of benchmark studies upon which the decision can be based.

The one-electron Kohn-Sham orbitals are determined by

$$\hat{h}^{KS}\varphi_i = (-\tfrac{1}{2}\nabla^2 + V_S)\varphi_i = \varepsilon_i\varphi_i \tag{2.7}$$

where $\hat{h}^{KS}$ is the one-electron Kohn-Sham Hamiltonian operator, which consists of a kinetic energy operator and the Kohn-Sham potential V_S. This potential comprises the potential V_{Ne} due to the charged nuclei, an effective Coulomb potential V_C due to the charge density and an exchange-correlation potential V_{XC}. The Kohn-Sham operator works on the one-electron Kohn-Sham orbitals φ_i, and the corresponding ε_i can be interpreted as the orbital energies of φ_i. Although these orbitals were originally developed only to construct the density, they appear to be suitable for qualitative chemical application.[145-148] The Kohn-Sham equations have to be solved iteratively, since, in order to obtain the orbitals, one needs the density, which is constructed from the very same orbitals. This is done using the self-consistent field (SCF) procedure. Starting from an initial guess of the density, the potentials are calculated and the Kohn-Sham equations are solved, yielding a set of orbitals from which a (hopefully) improved density is constructed. This procedure is repeated until the difference between the input density and output density drops below a specified threshold: the density is then approximately self-consistent and the computation converged to within certain criteria.

2.4 Computational Details

All computations within this thesis are based on density functional theory (DFT),[141,142] and have been carried out using the Amsterdam Density Functional program, developed by Baerends and co-workers,[149-151] and the Quantum-regions Interconnected by Local Descriptions (QUILD) program.[152-154] The numerical integration is performed using the procedure developed by Te Velde *et al.*[155,156] For some of the potential energy surfaces in chapter 4, the fuzzy cells integration scheme developed by Becke[157] was applied, as implemented in the ADF2013 release.[158] The molecular orbitals (MOs) are expanded in a large uncontracted set of Slater-type orbitals (STOs), no Gaussian functions are involved. This

basis set, denoted TZ2P, is of triple-ζ quality for all atoms and has been augmented with two sets of polarization functions.[159] The polarization functions are 2p and 3d on H, 3d and 4f on C, N, O, F, P and Cl, 4d and 4f on Br and 5d and 4f on I. For the transition metals, the polarization functions are 4p and 4f on Co, Ni, Cu, 5p and 4f on Rh, Pd and Ag and 6p and 5f on Ir, Pt and Au. An auxiliary set of s, p, d, f and g STOs is used to fit the molecular density and to represent the Coulomb and exchange potentials accurately in each self-consistent field (SCF) cycle. For the work on catalysis (chapters 3 to 7), all electrons are included in the variational treatment. For the work on halogen bonds in chapters 8 and 9, a frozen core approximation is applied. In these studies, the core shells comprised the 1s for C, N, O and F; 1s2s2p for Cl and K; up to 3p for Br and up to 4p for I.

Equilibrium structures and transition state geometries are obtained by optimizations using analytical gradient techniques.[160] Geometries and energies are calculated using functionals based on the generalized gradient approximation (GGA). For all chapters, except chapter 8, the BLYP functional is used, in which exchange is described by Slater's Xα potential,[161] with nonlocal corrections due to Becke[162,163] added self-consistently. Correlation is treated using the gradient-corrected functional of Lee, Yang and Parr.[164] The results in chapter 8 are obtained with the BP86 functional, using again Becke's corrections[162,163] on Slater's Xα potential,[161] but the correlation is now treated using the Vosko-Wilk-Nusair (VWN) parameterization[165] with nonlocal corrections due to Perdew[166] added, again, self-consistently.[167]

For a number of studies, mainly those in chapters 4, 5 and 9, dispersion interactions are included by means of additional corrections to the functional. In chapters 4 and 5, Grimme's third generation DFT-D3 method is applied.[168] In this approach, the density functional is augmented with an empirical term correcting for long-range dispersion effects, described by a sum of damped interatomic potentials of the form C_6R^{-6} added to the usual DFT energy. In chapter 9, the DFT-D3(BJ) method is applied,[169] which is a revised version of the DFT-D3 method, with a damping function of the form $C_6/(R^6+c)$ as proposed by Becke and Johnson.[170] Scalar relativistic effects are accounted for using the zeroth order regular approximation (ZORA).[171,172] These approaches have all been carefully tested and agree well with experimental results or high-level coupled cluster reference data.[113,161-166,173-182]

Energy minima and transition states have been verified through vibrational analysis,[183-185] except for the quadruplexes in chapter 9. All minima were found to have zero imaginary frequencies, whereas all transition states have one. The character of the normal

mode associated with the imaginary frequency has been analyzed to ensure it resembles the reaction under consideration. In a number of instances intrinsic reaction coordinate (IRC) calculations[186,187] have been performed to obtain the potential energy surface (PES) of the chemical process. In some cases, these potential energy surfaces have been approximated by means of the Transition-Vector Approximation to the IRC (TV-IRC). In this approach, the PES around the transition state is approximated using the transition vector, that is, the normal mode associated with a negative force constant leading from the saddle point on the PES to the steepest descent paths.[188] The PyFrag program was used to facilitate the analyses along the PES.[189]

Throughout this thesis, the focus lies on the electronic energies of the molecular systems. In a number of instances (mainly chapters 6 and 8), enthalpies or Gibbs free energies at 298.15 K and 1 atm. have been calculated using standard statistical mechanics relationships, and the computed partition functions, assuming an ideal gas.[138,190] The thermodynamic effects were found to have only a small influence on the energies and do not alter any of the encountered trends. It should be noted, however, that small barriers for either the forward or backward reaction that are present on the electronic potential energy surface, may vanish when thermodynamic effects are taken into account. For clarity, the results are therefore not discussed, but available in the supplementary information of the publications corresponding to these chapters.

The distribution of the electron density is analyzed using the Voronoi deformation density (VDD) method[191,192] for computing atomic charges. Within this method, the atomic charge on an atom A (Q_A^{VDD}) is computed as the integral of the deformation density in the volume of the Voronoi cell of atom A:

$$Q_A^{VDD} = -\int_{\substack{\text{Voronoi cell}\\ \text{of atom A}}} \left(\rho(r) - \sum_B \rho_B(r)\right) \mathrm{d}r \ . \tag{2.8}$$

The Voronoi cell of atom A is defined as the compartment of space bounded by the bond midplanes on, and perpendicular to, all axes between the nucleus of atom A and the nuclei of its neighboring atoms. The deformation density is the difference between the density $\rho(r)$ of the molecular system and the superposition of spherically averaged atomic densities $\rho_B(r)$ for neutral atoms B. The interpretation of VDD charges is rather straightforward: it measures how much charge flows out of ($Q_A^{VDD} > 0$) or into ($Q_A^{VDD} < 0$) the Voronoi cell of atom A, due to chemical interactions. Within a fragment-based approach, the VDD charge

of a molecular fragment can be calculated as the sum of the VDD charges of the individual atoms belonging to that fragment.

2.5 Activation Strain Model of Chemical Reactivity

The energy profile of a chemical process, that is, the change in energy of the molecular system as a function of the progress of the chemical process, can be obtained using, for example, density functional theory. However, to explain why molecular fragments interact, or react, requires a deeper understanding. The activation strain model of chemical reactivity[193-196] can be used to get insights into the features of an energy profile, and, for this purpose, has been applied in all research contained in this thesis. It is a fragment-based approach, dissecting the relative energy ΔE into two separate terms. For example, one can obtain insight into the height of the reaction barrier by splitting its energy, $\Delta E^{\ddagger}$, in the strain energy $\Delta E^{\ddagger}_{\text{strain}}$, and the interaction energy $\Delta E^{\ddagger}_{\text{int}}$:

$$\Delta E^{\ddagger} = \Delta E^{\ddagger}_{\text{strain}} + \Delta E^{\ddagger}_{\text{int}} \,. \tag{2.9}$$

The strain energy $\Delta E^{\ddagger}_{\text{strain}}$ is the energy required for the geometrical deformation of the fragments from a reference geometry (often, but not necessarily, their equilibrium geometry) to the geometry they acquire at the transition state. It is therefore strongly related to the structural rigidity of the fragments. Since the reference geometries are usually not distorted, this term is typically destabilizing. It can gain significant values when deformations are large, such as the substrate undergoing bond cleavage during oxidative addition. However, for the formation of metal-ligand bonds M–L, such as discussed in chapter 3, or some of the DX···A$^-$ halogen bonds in chapter 8, there is only a moderate change in the geometry of the ligand, or DX fragment, respectively. In these cases, the strain energy term is only moderately destabilizing. In principle, the strain term can also incorporate excitations to electronic configurations that are better suited or required for the interaction studied, but most often the reference fragments are chosen as already having the correct valence configuration.

The strain term can be split further into separate contributions from each fragment, as is done, for example, in some of the chapters on catalysis, where the contributions from catalyst deformation and substrate deformation are computed separately, to show that a significant part of the reaction barrier originates from the rigidity of the catalyst. Furthermore, note that in the formation of the metal-ligand bond M–L, as well as the DX···A$^-$

halogen bond formation, there is a monatomic fragment (M or A^-), for which the strain energy is zero by definition, because there are no possible geometric changes.

The interaction energy $\Delta E_{\text{int}}^{\ddagger}$ accounts for all chemical interactions as they arise when the deformed reactants are brought from infinity to their positions in the transition state geometry. This term can be further dissected using an energy decomposition scheme, of which there are several available. The EDA method[147,197,198] used within this thesis will be discussed in section 2.6.

The activation strain model can be generalized to any point along an energy profile.[193,194,199-202] The relative energy ΔE, as well as its components, then become functions of the reaction coordinate ζ and Equation 2.9 generalizes to

$$\Delta E(\zeta) = \Delta E_{\text{strain}}(\zeta) + \Delta E_{\text{int}}(\zeta) \ . \tag{2.10}$$

When applied to an energy profile of a chemical reaction with a central reaction barrier, as for example encountered for most oxidative addition reactions in this thesis, all terms start at a value close to zero, but not necessarily at zero. This is because a reaction (in the gas phase) typically starts from a precursor complex, in which the fragments are slightly distorted (small ΔE_{strain}) and interact only weakly (small ΔE_{int}). From there on, the reactants become increasingly deformed along the reaction coordinate, leading to a continuously increasing strain energy ΔE_{strain}. Concomitantly, the interaction between the fragments usually strengthens, which leads to the interaction energy ΔE_{int} becoming more stabilizing along the reaction profile. At the point where the destabilization from the strain term increases at the same rate as the stabilization from the interaction energy term strengthens, that is, $dE_{\text{strain}}/d\zeta = -dE_{\text{int}}/d\zeta$, the derivative of the total energy profile with respect to the reaction coordinate is zero ($dE/d\zeta = 0$). At this point, the energy profile achieves either a maximum (the reaction barrier), where the transition state occurs, or a stable minimum.

It follows that, to elucidate the height of a reaction barrier, or the stability of a stationary point, one should not only consider the rigidity of the fragments and the strength of their mutual interaction, but also the position along the reaction coordinate, and therefore the slopes of the strain and interaction terms. Depicted in Figure 2.1 is a comparison of the activation strain analyses of two generic chemical reactions to exemplify this. In this comparison, the strain curves ΔE_{strain} resulting from both reactions are chosen to be equal, while the interaction curves ΔE_{int} are different. From this figure, it is easily concluded that, upon going from the first reaction (black lines) to the second reaction (red lines), the energy profile $\Delta E(\zeta)$ is shifted up in energy, due to a weaker interaction between the fragments. This

results in a higher reaction barrier, which is shifted to the product side because the interaction energy curve is descending less steeply. This is in agreement with the Hammond postulate,[203] which indeed follows naturally from the activation strain model. Note, however, that an analysis at the transition state geometries only, as indicated by the dashed lines in Figure 2.1, can be misleading, as in this case one would conclude that the reaction barrier becomes higher due to a significant increase in strain energy, and even despite (!) a slightly more stabilizing interaction between the fragments.

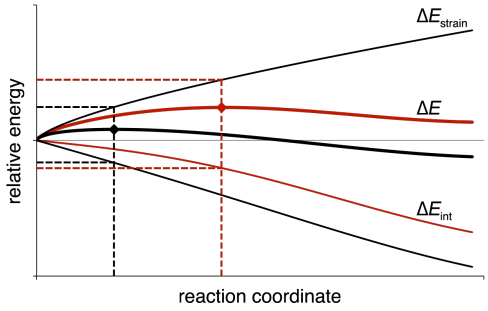

Figure 2.1 Comparison of generic activation strain analyses of two different reactions.

Although analyses along full reaction paths (or critical sections thereof) are more insightful than single point analyses at the transition state only, there are still a number of important factors to take into account in order to avoid misleading results. Firstly, analyses of two similar reactions are more readily compared when the energy profiles are projected onto a critical geometrical parameter. This parameter should be well-defined along the reaction profile and be sufficiently descriptive for the overall reaction process, but also undergo considerable changes in the transition state region.[188] Secondly, within this model, the total energy profile results from two opposing contributions, but these contributions are not orthogonal and thus influence each other. The strain term, for example, is almost always positive as a consequence of its very definition. Eliminating the strain term by freezing the geometries of the fragments and pushing them towards each other, however, would not lead to a lower total energy profile. Instead, the interaction term would weaken and, since it includes a repulsive component as well, eventually become repulsive, likely raising the total energy profile to higher values than the initial energy profile that was obtained with relaxed geometries. Thus, a significant part of the interaction energy that is built up during the

reaction, requires a certain amount of geometrical deformation, and thereby strain energy. This balance between mutually dependent terms usually does not cause problems, but should be kept in mind when applying any model that contains interacting and opposing components. To get insight into the importance of this interplay, it can be useful to use additional analyses where (part of) the geometries are fixed. In chapters 3 and 5 the geometries of the fragments are entirely fixed in the analyses of the bonding interactions as function of the ligand-metal-ligand angle. This is done to prevent any perturbation stemming from geometry changes of the fragments that could easily hide the small, though significant, variations in the components of the bonding mechanism that occur when the ligand-metal-ligand angle is varied.

So far, the activation strain model is discussed in the context in which it is most often applied, namely bimolecular reactions via a transition state, such as oxidative additions, as in this thesis, S_N2 reactions[193,204-206] or pericyclic reactions.[207,208] The model is, however, equally useful for the analyses of barrier-free bond formations, such as the hydrogen and halogen bonds discussed in chapters 8 and 9, and has also been generalized to study unimolecular processes.[209-211]

2.6 Molecular Orbital Theory & Interaction Energy Decomposition

The activation strain model reveals great insight into relative energies and even entire reaction energy profiles, as it provides the very relevant question *why* a certain geometrical deformation leads to an energetic destabilization, or *why* molecular fragments can build up a particular mutual interaction. Thus, to achieve a genuine explanation of the phenomena of interest, the reasons behind the changes in strain and interaction energy can be subjected to further investigation. In the following chapters, both the strain energy and the interaction energy are further analyzed, often using (Kohn-Sham) molecular orbital (MO) theory.[212-215]

As discussed in the previous section, the strain energy of a fragment is the energy needed for the geometric deformations, relative to a reference geometry. Since this reference geometry is typically the equilibrium geometry of the fragment, the amount of strain energy is often directly related to the amount of geometrical distortion, and can be readily linked to the extent to which, for example, bonds are stretched or angles have changed. Further explanation is therefore not always needed. However, when required, MO theory can help to understand why a certain geometric deformation leads to a less stable molecular

species. This is because changes in the total energy of the molecular fragment tend to parallel the changes in the sum of its orbital energies, and the orbital energies are again altered by changes in the molecular geometry. Thus, by investigating the dependence of the orbital energies on a geometrical parameter of interest, as is done in Walsh diagrams, one can explain why a certain molecular deformation leads to a destabilization of the molecular fragment. In a subsequent step, one can of course divide the fragment itself into smaller fragments, and provide an explanation for, for example, a rise in the orbital energy in terms of a decreased in-phase or increased out-of-phase overlap of the orbitals on the smaller fragments. Likewise, a lowered orbital energy can be ascribed to an increased in-phase overlap or decreased out-of-phase overlap. This process can be repeated until the explanation is provided in terms of atomic orbitals, which no longer have any geometry dependence. Often, however, a satisfactory level of understanding is achieved already at an earlier stage, based on the transferability of properties of common functional groups.

Studying the how and why of chemical interactions between molecular fragments is, in essence, chemical bond analysis, and constitutes a core aspect of this thesis, and theoretical chemistry in general. In the following chapters, the interaction energy is usually split into separate terms arising from different types of interactions, to get a quantitative idea of their contributions to the total interaction energy. This is done using the energy decomposition analysis (commonly abbreviated EDA) scheme as implemented in the ADF software suite.[147,149] This scheme is chosen for its transparent, easy-to-understand nature, as it dissects the interaction energy into terms that directly correspond to concepts from MO theory, thus revealing causal bonding mechanisms. The approach is based on that of Morokuma[216,217] and the extended transition state (ETS) method developed by Ziegler and Rauk.[197,198,218] Within this scheme, the interaction energy ΔE_{int} is decomposed into three terms, which can be interpreted physically in the framework of the molecular orbitals (MOs) arising from Kohn-Sham DFT:

$$\Delta E_{\text{int}} = \Delta V_{\text{elstat}} + \Delta E_{\text{Pauli}} + \Delta E_{\text{oi}} \,. \tag{2.11}$$

Similar to the generalization of the ΔE_{int} term to any point along an energy profile (as discussed in section 2.5, see Equations 2.9 and 2.10) also this equation can be generalized to the entire reaction profile. Each term then becomes a function of the reaction coordinate ζ.

For the discussion of the individual terms contributing to the interaction energy ΔE_{int}, the formation of AB is considered from two fragments A and B, which, as discussed in the previous section, already have the geometry and electronic configuration corresponding to

the combined complex AB. These fragments have electronic densities ρ_A and ρ_B, with corresponding wavefunctions Ψ_A and Ψ_B and energies E_A and E_B. The first term, ΔV_{elstat}, is the classical electrostatic interaction between the fragments as they are brought from infinity to their positions in the complex AB, giving rise to the sum density $\rho_{A+B} = \rho_A + \rho_B$, and corresponding Hartree product wavefunction $\Psi_A\Psi_B$. It consists of the Coulombic repulsion between the nuclei α and β (at positions R, with charges Z) of the fragments A and B, respectively, as well as the repulsion between their unperturbed electron densities ρ_A and ρ_B, and the attractive interactions between the nuclei of one fragment with the electron density of the other fragment:

$$\begin{aligned}\Delta V_{elstat} = & \sum_{\alpha \in A} \sum_{\beta \in B} \frac{Z_\alpha Z_\beta}{R_{\alpha\beta}} \\ & - \int \sum_{\alpha \in A} \frac{Z_\alpha \rho_B(r)}{|R_\alpha - r|} dr - \int \sum_{\beta \in B} \frac{Z_\beta \rho_A(r)}{|R_\beta - r|} dr \\ & + \int\int \frac{\rho_A(r_1)\, \rho_B(r_2)}{r_{12}}\, dr_1\, dr_2 \ .\end{aligned} \tag{2.12}$$

It is known from elementary electrostatics that two interpenetrating charge clouds have a repulsion that is smaller than the one between point charges at their centers, from which follows that fragments consisting of electronic densities around positive nuclei will typically experience a net attraction. Thus, ΔV_{elstat} is usually attractive for molecular fragments at chemically relevant distances. For discussions in later sections, it is important to note that this term is computed from frozen electron densities ρ_A and ρ_B, obtained by optimizations in absence of the other fragment.

The Pauli repulsion, ΔE_{Pauli}, is the energy change that occurs upon going from the product wavefunction $\Psi_A\Psi_B$ to an intermediate wavefunction Ψ^0 that, after antisymmetrization by an operator $\mathcal{A}$ and renormalization by a constant N, properly obeys the Pauli principle: $\Psi^0 = N\mathcal{A}\{\Psi_A\Psi_B\}$. This intermediate state, with density ρ^0, has energy E^0, such that $\Delta E^0 = E^0 - E_A - E_B = \Delta V_{elstat} + \Delta E_{Pauli}$ and $\Delta E_{Pauli} = \Delta E^0 - \Delta V_{elstat}$. The Pauli repulsion comprises the repulsive interaction between electrons having the same spin. It is responsible, for example, for the 4-electron destabilizing interactions between doubly occupied orbitals from the different fragments. This is the origin of steric repulsion: when two occupied valence orbitals from different fragments overlap, antisymmetrization results in a nodal plane.

The large gradients in this region lead to a significant increase in the kinetic component of the orbital energies (Equation 2.7).

In the final step of the bond formation between fragments A and B, the system is allowed to relax from Ψ^0, and corresponding ρ^0, to the final Ψ^{AB} and optimized density ρ of the molecular complex AB. The accompanying energy change is the orbital interaction term: $\Delta E_{oi} = E^{AB} - E^0$. This term is by definition stabilizing, because it involves an optimization. More specifically, it allows the virtual orbitals on the fragments to be mixed in. As a result of this mixing, the orbital interaction component contains the stabilizing contributions from polarization of the fragments A and B, as well as charge transfer between the fragments. It is hard, if not impossible, to rigorously distinguish polarization from charge transfer, and this is therefore not attempted in this interaction energy decomposition scheme (in contrast to the scheme of Morokuma[216,217]). However, when using a fragment-based approach and further orbital analyses, it is possible to get insight into the two individual contributions at least partially. Both polarization and charge transfer will show up as occupied-virtual orbital mixing, but in the case of polarization, the occupied and virtual orbitals will be localized on the same fragment, whereas charge transfer will show up as the mixing of occupied orbitals on one fragment with unoccupied orbitals on the other fragment. When using very large basis sets, care must be taken since the basis functions of one fragment can extend into the domain of the other fragment. Besides detailed orbital analyses, additional electron density analyses (based on atomic charge analyses, the deformation density, etc.) can be helpful to distinguish polarization from charge transfer.

Furthermore, it follows from group theory that only orbitals of the same symmetry, that is, having the same character under the available symmetry operations, can interact and mix. This allows for a further decomposition of the total orbital interaction energy ΔE_{oi} into contributions from each irreducible representation (irrep) Γ of the point group of the molecular system:[198]

$$\Delta E_{oi} = \sum_{\Gamma} \Delta E_{oi}^{\Gamma} . \tag{2.13}$$

Finally, when the functional is augmented with an explicit correction to account for dispersion interactions, the contribution ΔE_{disp} from this term can simply be added to Equation 2.11 as an additional component of the interaction energy ΔE_{int}.

In Figure 2.2, schematic orbital interaction diagrams are shown for the different types of orbital interactions that play a main role throughout the following chapters.

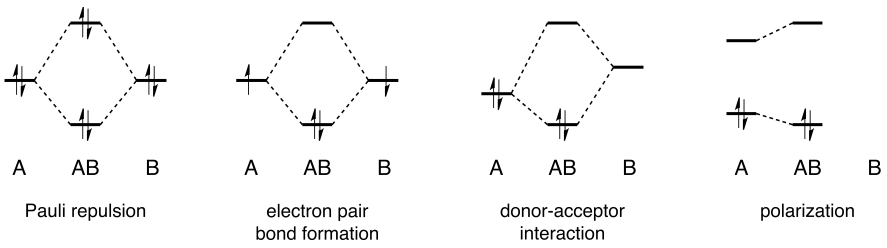

Figure 2.2 Orbital interaction diagrams for the interactions most commonly appearing throughout this thesis.

There are many other schemes available that divide the interaction energy into separate terms,[219-227] and one could argue that some of them give more realistic representations of, for example, the electrostatic attraction between fragments. Also, the Pauli repulsion term has been criticized for being based on an "*arbitrarily chosen, non-physical reference state*", and resulting from "*first violating the Pauli principle and then imposing it*".[210,228-230] Such statements may, at times, be relevant reminders for the overenthusiastic user of the decomposition scheme, but serve no further purpose: the scheme is a quantitative analysis tool that, preferably accompanied by results from additional analyses, assists in explaining a certain result using MO theory. All terms are defined as they are, and produce the numbers that follow from these clear and transparent definitions. The results provided by the decomposition scheme should therefore not be interpreted as the final answer to a question, nor be presented as such.

After this rigorous numerical treatment, the explanations in this thesis are often presented schematically, using generic hydrogen-like atomic orbitals and a few core concepts from MO theory, further aided by symmetry considerations derived from group theory. A number of elementary atomic properties, such as electronegativity and atomic radii, can easily be taken into account using what is in essence a perturbative treatment. Thus, although the results are derived from state-of-the-art DFT computations and detailed analyses, the final explanation often shows the essence of the phenomenon of interest in a pictorial manner that is easy to memorize, to communicate and to apply to new situations. Such representations nevertheless accurately account for the observations made, and provide important insights. In the past, this approach, and MO theory in general, has proven to be a very powerful tool for explaining many observations made in a variety of fields in chemistry, limited not only to molecules, but also including solids.[212-215,231]